AN UNMIXING-BASED FRAMEWORK FOR IMPROVING THE SPATIAL RESOLUTION OF LAND SURFACE TEMPERATURE PRODUCTS

Moussa Sofiane Karoui, *Fatima Zohra Benhalouche*, *Farah Benharrats* and *Habib Mahi*

Agence Spatiale Algérienne, Centre des Techniques Spatiales, Arzew, Algeria

ABSTRACT

Land Surface Temperature (LST) products derived from a thermal infrared sensor typically suffer from Low-spatial Resolution (LR). In this paper, a novel framework, which leverages the linear spectral unmixing concept applied to Visible, Near and Shortwave InfraRed (VNIR–SWIR) spectral bands, with Intermediate/Low-spatial Resolution (ILR), acquired by sensors on the same platform, is proposed to improve the spatial resolution of the LST product. More precisely, obtained ILR fractional abundances are employed, initially, in a robust estimation using iteratively reweighted least squares to retrieve class temperatures at the LR scale. On the other hand, obtained ILR fractional abundances are also used to derive, using a simulated annealing-based approach, a land cover classification map at a High-spatial Resolution (HR) scale. Then, a HR LST product is reconstructed by means of the retrieved class temperatures and the obtained HR land cover classification map. Multi-scale consistency is enforced through aggregation-disaggregation of residuals, modulated by edge-preserving weights derived from spatial gradients of the HR land cover classification map and entropy measures of the ILR fractional abundances. The proposed framework is validated, by means of geolocated in-situ temperature measures, on Landsat-9 Level-2 VNIR–SWIR data and LST product. Moreover, obtained results are also compared to those derived by some tested literature approaches. These conducted experiments clearly demonstrate the effectiveness of the proposed framework.

Index Terms— Land surface temperature, spatial resolution improvement, linear spectral unmixing, iterative reweighted least squares, simulated annealing, edge-preserving filtering, multi-scale downscaling.

1. INTRODUCTION

Land Surface Temperature (LST) is a critical variable in Earth observation. It is used for monitoring urban heat islands, assessing droughts, modeling evapotranspiration, and studying climate change. Many spaceborne platforms, such as Landsat-9, are equipped with, in addition to optical sensors, thermal infrared ones that provide valuable LST products. However, such a product is often provided at Low-spatial Resolution (LR) scale, e.g., 30 meters for the Landsat-9 Level-2 LST product, whereas optical spectral bands may reach an Intermediate/Low-spatial Resolution (ILR), e.g., 15 meters for the Landsat-9 Visible, Near and Shortwave InfraRed (VNIR–SWIR) pansharpened spectral bands. This low-spatial resolution mismatch limits the usefulness of LST products for fine-scale applications, especially in heterogeneous urban or agricultural environments [1], [2].

During previous years, various thermal sharpening (or downscaling) methods have been developed for improving the spatial resolution of LST products. Classical approaches, such as TsHARP [3] and DisTrad [4], establish statistical relationships between LR LST and ILR proxies, e.g., Normalized Difference Vegetation Index (NDVI), then apply these relationships at the ILR scale with residual corrections to maintain multi-scale consistency [5], [6]. More recent methods employ machine learning, e.g., random forests and neural networks, for nonlinear regression [7], [8] or physics-based approaches [9].

Despite their popularity, existing methods often treat the downscaling problem as a global regression task. This can result in the neglect of sub-pixel heterogeneity due to large-scale mixed pixels. The Linear Spectral Unmixing (LSU) concept, which consists in linearly decomposing observed pixels into their pure endmember spectra and fractional abundances [10], offers a rigorous method for capturing this heterogeneity. When applied to VNIR–SWIR spectral bands, in particular acquired on the same platform as the thermal infrared sensor, LSU may provide information about surface composition at ILR and High-spatial Resolution (HR) scales.

In this investigation, a novel framework is proposed to improve the spatial resolution of LST products. This framework leverages the LSU concept, based on Nonnegative Matrix Factorization (NMF) [11] and addresses spectral variability [12], applied to ILR VNIR–SWIR spectral bands, in particular, acquired by sensors on the same platform that supplies the LST product.

More specifically, obtained ILR fractional abundances are first used in a robust estimation using Iteratively Reweighted Least Squares (IRLS) [13] to retrieve class temperatures at the LR scale. Moreover, these obtained ILR fractional abundances are also used to derive, using a Simulated Annealing (SA)-based approach [14], a land cover classification map at a HR scale. Then, a HR LST product is reconstructed by means of the retrieved class temperatures and the obtained HR land cover classification map. Multi-scale consistency [3] is enforced through aggregation-disaggregation of residuals, modulated by edge-preserving weights derived from spatial gradients of the HR land cover classification map and entropy measures of the ILR fractional abundances.

This paper is structured as follows. In Section 2, the proposed framework is presented. Section 3 involves experiments performed with Landsat-9 Level-2 VNIR–SWIR data and LST product. Finally, Section 4 concludes this investigation.

2. PROPOSED FRAMEWORK

As introduced, the proposed framework is intended to improve the spatial resolution of a LR LST product. It operates in five stages described hereafter.

1) The LSU stage that consists in estimating fractional abundances from ILR optical VNIR–SWIR image provided by the same platform that supplies the considered LST product. In this investigation, the NMF-based approach, which deals with spectral variability and associated with the modified Augmented Linear Mixing Model (mALMM), described in [12] is used to estimate fractional abundances at the ILR scale. As a reminder, mALMM, which captures spectral variations through multiple nonnegative additive terms, models the relationship between the observed VNIR–SWIR image, the endmembers and fractional abundances as follows

$$y_i = M\, diag(\Phi_i)\alpha_i + u_i - l_i, \quad (1)$$

where $y_i \in \mathbb{R}_+^{L\times 1}$, with $i = 1\dots P$, denotes the nonnegative spectrum associated with a given pixel i of the observed image. L and P are, respectively, the number of spectral bands and the number of pixels. The nonnegative matrix $M \in \mathbb{R}_+^{L\times N}$, where N is the number of endmembers, contains, in its columns, endmember spectra (each column represents one endmember spectrum). Moreover, the nonnegative vector $\alpha_i \in \mathbb{R}_+^{N\times 1}$ ($\alpha_i = [\alpha_{i,1}, \dots, \alpha_{i,N}]^T$) contains fractional abundances of endmembers in the considered pixel i. Furthermore, the nonnegative vector $\Phi_i \in \mathbb{R}_+^{N\times 1}$ contains scaling factors, which allow scaling adjustments of each endmember in the considered pixel i. Thus, $diag(\Phi_i)$ is a nonnegative diagonal matrix, of dimension $N \times N$, that contains the vector Φ_i in its diagonal. The nonnegative vector $u_i \in \mathbb{R}_+^{L\times 1}$ (respectively $l_i \in \mathbb{R}_+^{L\times 1}$) contains nonnegative upper (respectively lower) deviations that account for spectral variations, at the considered pixel i, relative to some reference observations. In addition, the following well-known sum-to-one constraint is considered

$$\sum_{j=1}^{N} \alpha_{i,j} = 1. \quad (2)$$

At this stage, the initial nonnegative matrix M of endmember spectra may be estimated by the approach described in [15], while all initial fractional abundances may be estimated by the fully constrained least squares method [10]. Then, these spectra and abundances are iteratively updated by means of the NMF-based algorithm described in [12].

2) The fractional abundances aggregation stage, which consists in simply aggregating all estimated ILR fractional abundances α_i, with $i = 1\dots P$, at the LR scale. Therefore, at this stage, LR fractional abundances, denoted $\beta_{i'}$, with $i' = 1\dots P'$ (P' denotes the number of pixels of the LR LST product), are obtained, while maintaining the sum-to-one constraint (2), i.e., $\sum_{j=1}^{N} \beta_{i',j} = 1$.

3) The land cover classification map creation stage that consists in deriving a HR land cover classification map by means of all estimated ILR fractional abundances α_i, with $i = 1\dots P$. At this stage, the SA-based approach described in [14] is used to produce such a HR classification map, which consists of P'' pixels (with $P' \leq P < P''$).

4) The class temperatures estimation stage, which consists in estimating class temperatures T_j, with $j = 1\dots N$, from all LR $LST_{LR_{i'}}$ pixels by means of all obtained aggregated LR fractional abundances $\beta_{i'}$. In this investigation, $LST_{LR_{i'}}$, at the pixel i', with $i' = 1\dots P'$, is considered as a linear combination of all class temperatures T_j weighted by the aggregated LR fractional abundances $\beta_{i'}$ at the considered pixel i' as follows

$$LST_{LR_{i'}} = \sum_{j=1}^{N} \beta_{i',j}\, T_j. \quad (3)$$

Thus, in this investigation, each endmember is considered to have a fixed temperature in the complete imaged scene.

At this stage, the considered class temperatures T_j, with $j = 1\dots N$ are estimated by means of IRLS technique [13]. This is achieved by solving the following optimization problem

$$\min_{T_1,\dots,T_N} \sum_{i'j} \rho_H\,(LST_{LR_{i'}} - \sum_j \beta_{i',j}\, T_j) + \lambda \sum_j (T_j - T_j^{prior})^2, \quad (4)$$

where ρ_H is the Huber regularization parameter, λ is an optional regularization weight, with T_j^{prior} optional prior constraints (e.g., physical bounds: for instance, 250 Kelvins $\leq T_j \leq$ 350 Kelvins). The solution of the above optimization problem yields class temperatures that are consistent with the observed LST at the LR scale.

5) The HR LST reconstruction stage that consists in retrieving the LST product at the HR scale with P'' pixels. This is achieved, at this stage, firstly by simply combining the estimated class temperatures and produced HR land cover classification map: each pixel class, in the HR classification map, is replaced by the corresponding estimated class temperature. This leads to a first reconstructed HR LST denoted $LST_{HR,0}$. Then, multi-scale consistency is enforced through aggregation-disaggregation of residuals, modulated by edge-preserving weights derived from spatial gradients of the HR land cover classification map and entropy measures of the ILR fractional abundances. The residual $Res_{LR_{i'}}$, for the pixel i', at the LR scale is computed as follows

$$Res_{LR_{i'}} = LST_{LR_{i'}} - Agg\big(LST_{HR,0}\big)_{i'}, \quad (5)$$

where Agg denotes the aggregation operator of the first reconstructed $LST_{HR,0}$ (the aggregation considers each HR pixels block corresponding to the LR pixel i'). This residual is then interpolated to the HR scale, obtaining thus Res_{HR}, and applied with edge-aware weighting as follows to obtain a new HR LST, denoted $LST_{HR,1}$

$$LST_{(HR,1)_{i''}} = LST_{(HR,0)_{i''}} + w_{edge_{i''}}\, w_{ent_{i''}}\, Res_{HR_{i''}}, \quad \text{with } i'' = 1 \dots P'', \quad (6)$$

where edge weighting $w_{edge_{i''}}$ is derived from the spatial gradient of the HR classification map as follows

$$w_{edge_{i''}} = 1 - norm\left(\nabla ClassMap_{HR_{i''}}\right), \quad (7)$$

where $norm(\nabla ClassMap_{HR})$ denotes the normalized spatial gradient magnitude of the HR classification map. Here, regions with sharp class boundaries have lower weights, preserving discontinuities. Entropy weighting $w_{ent_{i''}}$ is computed by means of interpolated, at the HR scale (while preserving the sum-to-one constraint (2)), ILR fractional abundances as follows

$$w_{ent_{i''}} = 1 - \frac{Entropy\left(\left\{\alpha_{1_{i''}}, \ldots, \alpha_{N_{i''}}\right\}\right)}{\log N}. \quad (8)$$

Here, pure pixels, with low entropy, receive full correction, whereas mixed pixels receive partial correction.
Optionally, a refined reconstructed HR LST product, denoted $LST_{HR,2}$, may be obtained by edge-preserving refinement using a bilateral filter, while respecting sharp edges, applied to $LST_{HR,1}$.

3. EXPERIMENTAL RESULTS

In this investigation, the proposed framework is tested on real VNIR–SWIR and LST data. The obtained results are compared, by means of geolocated in-situ temperature measures from meteorological stations [16], to those provided by the following literature approaches: Bilinear Interpolation (BI) technique, NDVI-based TsHARP [3] and DisTrad [4] methods.

3.1. Tested data

Landsat-9 Level-2 VNIR–SWIR and LST data are considered and tested in this work. More precisely, Landsat-9 pansharpened VNIR–SWIR spectral bands, with 15-m spatial resolution, and LST product, with 30-m spatial resolution (obtained by a TsHARP-like approach applied to a 100-m spatial resolution thermal infrared spectral band), are tested in this investigation. These data are acquired on October 25, 2025 (at 10:38 am) and cover the Oran region, Algeria (path/row: 198/035). From the complete data, two sub-regions are selected and considered for experiments: the first one covers Oran city, and the second one covers Arzew city. Each sub-region contains four major land cover classes: Sea/Water body, Urban, Vegetation, and Bare soil.

3.2. Obtained results

The proposed framework and the above-mentioned literature approaches are applied to the tested data. Here, it should be noted that the proposed framework has been tested to produce, from the LR LST with 30-m spatial resolution, a HR LST product with 5-m spatial resolution: i.e., the HR land cover classification map has been created with 5-m spatial resolution from fractional abundances with 15-m spatial resolution. Besides, the BI technique is used to produce a HR LST product with 5-m spatial resolution, while TsHARP and DisTrad methods produce reconstructed LSTs with the same spatial resolution as the VNIR–SWIR spectral bands (i.e., 15-m spatial resolution). Moreover, the considered in-situ temperatures are averages of those measured at 10:00 and 11:00 am. The following figures and tables illustrate the obtained results, clearly confirming the effectiveness of the proposed framework.

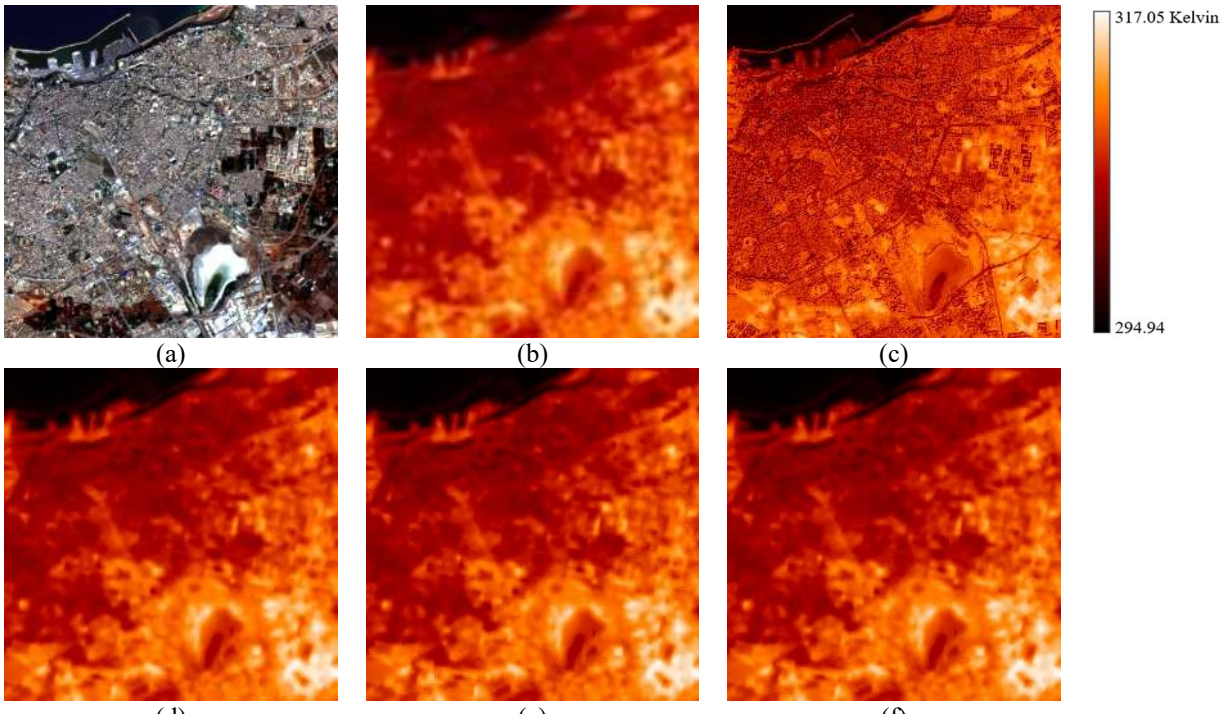


Figure 1. Oran city: (a) ILR 15-m RGB color composite, (b) initial LR 30-m LST, (c) estimated, by the proposed framework, HR 5-m LST, (d) estimated BI HR 5-m LST, (e) estimated TsHARP ILR 15-m LST, and (f) estimated DisTrad ILR 15-m LST.

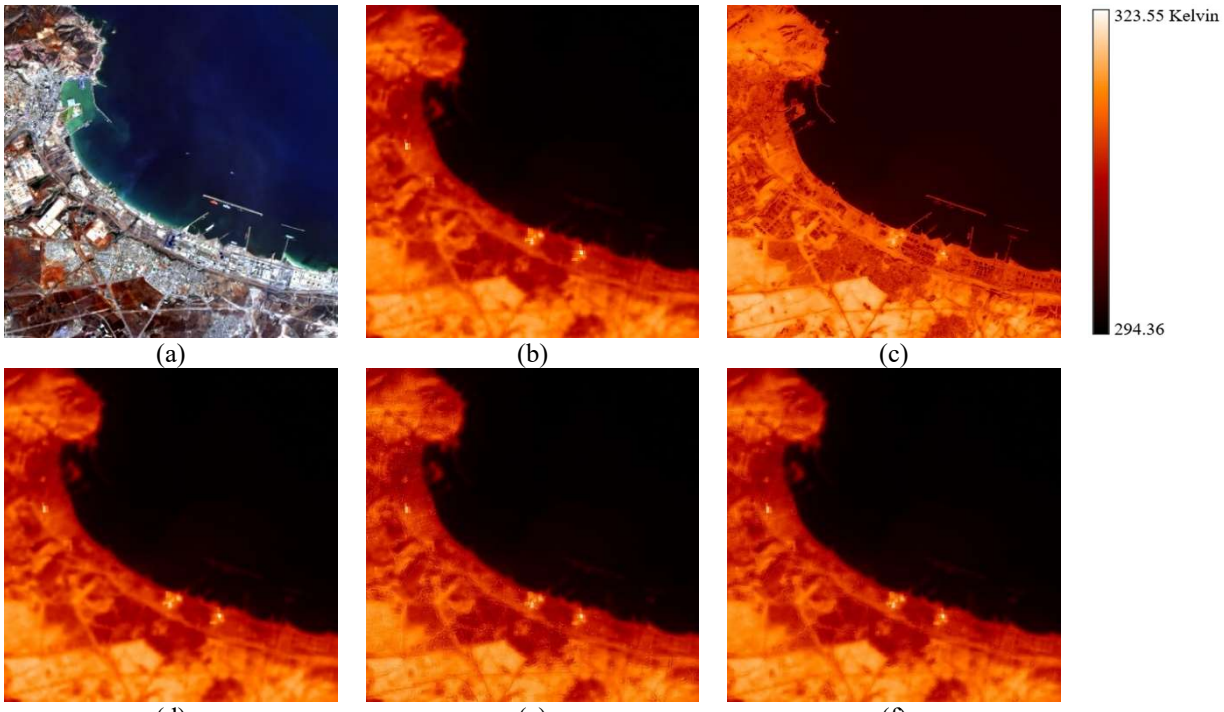


Figure 2. Arzew city: (a) ILR 15-m RGB color composite, (b) initial LR 30-m LST, (c) estimated, by the proposed framework, HR 5-m LST, (d) estimated BI HR 5-m LST, (e) estimated TsHARP ILR 15-m LST, and (f) estimated DisTrad ILR 15-m LST.

Table I. Estimated and in-situ (35.7103° N / 0.6528° W) temperatures for Oran city.

	Estimated temperature (Kelvin)	**In-situ temperature measure (Kelvin)**	**|Difference| (Kelvin)**
Original LST (30-m)	297.67	305.21	7.54
Proposed framework (5-m)	306.05		**0.84**
BI (5-m)	298.01		7.20
TsHARP (15-m)	298.43		6.78
DisTrad (15-m)	298.38		6.83

Table II. Estimated and in-situ (35.8477° N / 0.3073° W) temperatures for Arzew city.

	Estimated temperature (Kelvin)	**In-situ temperature measure (Kelvin)**	**|Difference| (Kelvin)**
Original LST (30-m)	304.77	300.77	4.00
Proposed framework (5-m)	299.90		**0.87**
BI (5-m)	305.08		4.31
TsHARP (15-m)	304.81		4.04
DisTrad (15-m)	305.14		4.37

4. CONCLUSION

In this investigation, a novel framework was proposed for improving the spatial resolution of LST products. This framework uses the linear spectral unmixing concept applied to visible, near and shortwave infrared spectral bands acquired by sensors on the same platform.

More precisely, estimated fractional abundances are used, initially, in a robust estimation by means of iteratively reweighted least squares to retrieve class temperatures. Furthermore, these fractional abundances are also used to derive, using a simulated annealing-based approach, a land cover classification map at a finer spatial resolution scale. Then, a high spatial resolution LST product is reconstructed by means of the retrieved class temperatures and the generated land cover classification map. Multi-scale consistency is enforced through aggregation-disaggregation of residuals, modulated by edge-preserving weights derived from spatial gradients of the land cover classification map and entropy measures of the estimated fractional abundances.

Based on the conducted experiments and obtained results, the proposed approach proves its efficiency in terms of improving the spatial resolution of LST products.

Future works may consist in testing the proposed framework on more Landsat-9 data, with cross-validation with other sensors' data. It would also be useful to test it for mapping urban heat islands at a finer spatial resolution.

5. REFERENCES

[1] Q. Weng, D. Lu, and J. Schubring, "Estimation of land surface temperature-vegetation abundance relationship," *Remote Sensing of Environment*, vol. 89(4), pp. 467–477, 2004.

[2] D. Roy, B. Das, P. Singh, P. Santra, S. Deb, B.K. Bhattacharya, A. Govind, R. Jatav, D. Sethi, T. Ghosh, J. Mukherjee, V.K. Sehgal, P.K. Jha, S. Goroshi, P.V.V. Prasad, and D. Chakraborty, "Assessing multi-model approaches for LST downscaling," *Nature Scientific Reports*, vol. 15(1), Article n° 10824, 2025.

[3] N. Agam, W.P. Kustas, M.C. Anderson, F. Li, and C.M.U. Neale, "A vegetation index based technique for spatial sharpening," *Remote Sensing of Environment*, vol. 107(4), pp. 545–558, 2006.

[4] C. Jeganathan, N.A.S. Hamm, S. Mukherjee, P.M. Atkinson, P.L.N. Raju, and V.K. Dadhwal, "Evaluating a thermal image sharpening model over a mixed agricultural landscape in India," *International Journal of Applied Earth Observation and Geoinformation*, vol. 13(2), pp. 178–191, 2011.

[5] H. Govil, S. Guha, A. Dey, and N. Gill, "Seasonal evaluation of downscaled land surface temperature: A case study in a humid tropical city," *Heliyon*, vol. 5(6), e01923, 2019.

[6] V.M. Bindhu, B. Narasimhan, and K.P. Sudheer, "Development and verification of a non-linear disaggregation method (NL-DisTrad) to downscale MODIS land surface temperature to the spatial scale of Landsat thermal data to estimate evapotranspiration," *Remote Sensing of Environment*, vol. 135, pp. 118–129, 2013.

[7] W. Yuan, S. Hu, C. Zhan, G. Wang, and Y. Luo, "Machine learning land surface temperature downscaling method based on Landsat 9 and Sentinel-2 satellite feature interaction," *Geo-spatial Information Science*, pp. 1–22, 2025.

[8] D. Hu, F. Guo, Q. Meng, U. Schlink, S. Wang, D. Hertel, and J. Gao, "A novel dual-layer composite framework for downscaling urban land surface temperature coupled with spatial autocorrelation and spatial heterogeneity," *International Journal of Applied Earth Observation and Geoinformation*, vol. 130, 103900, 2024.

[9] J.M. Norman, W.P. Kustas, and K.S. Humes, "Source approach for estimating soil and vegetation energy fluxes in observations of directional radiometric surface temperature," *Agricultural and Forest Meteorology*, vol. 77(3–4), pp. 263–293, 1995.

[10] J.M. Bioucas-Dias, A. Plaza, N. Dobigeon, M. Parente, Q. Du, and P. Gader, "Hyperspectral unmixing overview: Geometrical, statistical, and sparse regression-based approaches," *IEEE Journal of Selected Topics in Applied Earth Observations and Remote Sensing*, vol. 5(2), pp. 354–379, 2012.

[11] A. Cichocki, R. Zdunek, A.H. Phan, and S-I. Amari, *Nonnegative matrix and tensor factorizations: Applications to exploratory multi-way data analysis and blind source separation*. John Wiley and Sons, 2009.

[12] M.S. Karoui, F.Z. Benhalouche, and Y. Deville, "Hyperspectral unmixing with a modified augmented linear mixing model addressing spectral variability," *In 2022 IEEE Mediterranean and Middle-East Geoscience and Remote Sensing Symposium (M2GARSS)*, pp. 66–69, 2022.

[13] R. Chartrand and W. Yin, "Iteratively reweighted algorithms for compressive sensing," *In 2008 IEEE International Conference on Acoustics, Speech and Signal Processing (ICASSP)*, Las Vegas, NV, USA, pp. 3869–3872, 2008.

[14] A. Villa, J. Chanussot, J.A. Benediktsson, and C. Jutten, "Spectral Unmixing for the Classification of Hyperspectral Images at a Finer Spatial Resolution," *IEEE Journal of Selected Topics in Signal Processing*, vol. 5(3), pp. 521–533, 2010.

[15] M.S. Karoui, Y. Deville, S. Hosseini, and A. Ouamri, "Blind spatial unmixing of multispectral images: New methods combining sparse component analysis, clustering and non-negativity constraints," *Pattern Recognition*, vol. 45(12), pp. 4263–4278, 2012.

[16] Available online: https://power.larc.nasa.gov/data-access-viewer (accessed on 4 January 2025).